Gray-Box Modeling of a Pneumatic Servo-Valve

Farhad Toorani, Hosein Farahmandzad

Moghtader Engineering Company
Tehran, Iran
E-mail: toorani.farhad@gmail.com, h.farahmandzad@gmail.com

Mojtaba Aghamirsalim

Department of Electrical Engineering
Amirkabir University of Technology
Tehran, Iran
E-mail: mirsalim@aut.ac.ir

Abstract: This paper presents the evaluation as well as the combined analytical and experimental identification (gray box identification) of a servo-valve torque motor as the directional valve applied in a pneumatic actuator. Based on analytical modelling, a simple linear parametric model with transfer function and block diagram is developed. Next, the static and dynamic characteristics of the torque motor are obtained from experimental observations. The characteristics confirm the desired linear behaviour of the torque motor. Hence, linearized coefficients from a best curve fitting of static characteristics can be derived. Classical methods of identification are applied on the frequency and step responses obtained from a set of tests on the torque motor. Obtained tests results based on parsimony principle and model order of analytical investigations are then implemented to derive the best identified transfer function to describe the performance of the servo-valve torque motor. Design parameters are estimated with the comparison of the experimental and analytical models. These parameters can be implemented with acceptable accuracy for servo control studies of pneumatic actuators.

Keywords: pneumatic actuator; servo-valve; limited angle torque motor; gray box modeling

1 Introduction

Several advantages of pneumatic actuation systems over hydraulic and electromechanical actuation systems in positioning applications have caused their

wide application in industrial automation, motion control of materials and part handling, packaging machines, and in robotics. The advantages include low cost, cleanliness, ease of maintenance, and high power to weight ratio. The drawback is due to the compressible nature associated with gases and the high speeds, which make it more difficult to control.

An electro-pneumatic control valve plays an important role in a pneumatic actuator. Its characteristics influence remarkably the performance of the actuator. This power element with small-amplitude, the low power electrical signal provides a high response modulation in pneumatic power. The dynamic response, null shift, threshold, and hysteresis are the most critical parameters that strongly influence the dynamic and static characteristics of the pneumatic actuators [1]. Limited angle torques motors (LATMs) are one of the electromechanical transducers which, when integrated with nozzles, can be used as servo-control valves in either pneumatic or hydraulic actuators. They can serve as proportional displacement, force output, or both.

Hydraulic servo-valves as a vital part of hydraulic actuation systems have been studied in literature. In [2, 3], the influence of magnetic fluids on the dynamic characteristics of a hydraulic servo-valve has been simulated and tested. LATMs are implemented as limited-motion rotary actuators in many areas of measurement, control, and energy conversion applications through an angle of less than ±180º. In [4], [6] a form of LATM, which is based on Laws' relay principle [5], has been evaluated and analyzed. The performance of this kind of torque motor is based on polarized reluctance principle in which torque and EMF are produced based on flux-switching action of rotor saliencies on a permanent magnet flux. Many complex problems of Laws' relay in rotary and rectilinear versions [7, 8], have been restricted to design problems which contain static and dynamic characteristics, e.g. stiffness of permanent magnets and torque sensitivity with respect to current.

The design and control of a two-pole toroidally wound armature brushless direct-current LATM with application in the fuel control of gas-turbine engines has been presented in [9]. To achieve a robust position control of the motor, a PID controller with a closed-loop fuel controller has been implemented using DSP.

The construction of servo-valve studied in our research is a type of Laws' relay which contains two windings set up on two bobbins placed around the rotor as control coils. This structure lowers the physical size, and the bobbins play the role of position limiters. The stator contains two separated soft iron yokes and two permanent magnets with high flux densities. The main characteristics of the motor are its miniature size, the capability of the rotor to revolve only up to ±3º, short dynamic response time due to its low inertia and the high magnetic stiffness that is desirable in servo-valves, high reliability due to its simple construction and the high quality of magnetic material.

This paper presents a combined analytical (white box) and experimental (black box) modeling of a pneumatic servo-valve torque motor, based on an approximate mathematical model developed from design data and experimental measurements. The black box modeling approach is the basis of system identification which estimates dynamic response and transfer function parameters. This approach is simpler than solving the nonlinear partial differential equations of the structure, and is especially suitable for design studies of the control loop of the pneumatic actuator when used as an accurate position tracker. Based on classical methods of identification, the frequency and step responses of the tested motor have been fitted by a continuous transfer-function response. The unknown parameters of a mathematical model are derived according to the presented models. The experimental results show that the proposed models provide an accurate prediction of the behavior of servo-valve torque motors.

2 Laws' Relay Principles

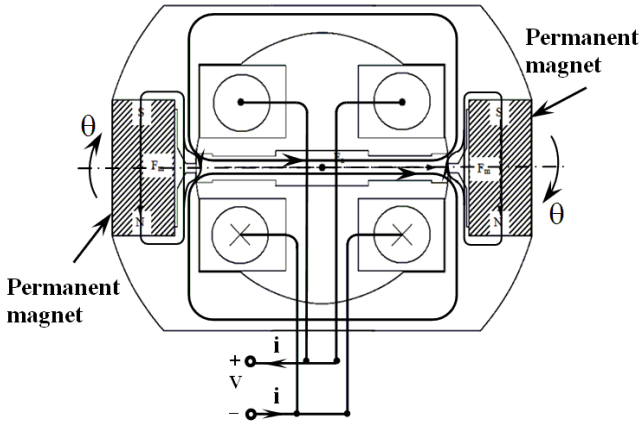

Figure 1
The schematic of Laws' relay servo-valve

A schematic of the tested torque motor is shown in Figure 1. It contains armature, two parallel coils, two permanent magnets, and yokes. Four core teeth overlap with armature and cause four variable air-gap reluctances, which make the motor act as a switch reluctance type. The two magnets tend to keep the armature in a null position ($\theta = 0$). With no external excitation, the flux density under each of the four teeth is equal and the low inertia of the rotor bridge poles causes a magnetic balance in the four air-gaps. By connecting a power source that can supply either unidirectional or bipolar current to the motor, an unbalance of flux density in the air-gaps is produced, which results in a new equilibrium of rotor

position. Inherently, the high stiffness of the magnet makes it like a spring with a stiffness torque proportional to the angular position. Since the torque produced by the flux of the control winding is proportional to the current (under non-saturated conditions), theses two components of the torque make the motor suitable for servo control systems and accurate positioning of a load connected to an actuator. A pneumatic nozzle is linked to the armature of the torque motor and the whole system acts as a directional-proportional valve that guides compressed air to cylinder chambers.

3 Mathematical Model of a LATM

The mathematical model of the Laws' relay system is based on the dynamic equations of motor which are described by the following differential equations.

$$\begin{aligned} & v-\left(\frac{\partial\lambda(i,\theta)}{\partial\theta}\right)\frac{d\theta}{dt}-\left(\frac{\partial\lambda(i,\theta)}{\partial i}\right)\frac{di}{dt}-Ri=0 \\ & \Rightarrow i(t)=\int\left[\left(\frac{\partial\lambda(i,\theta)}{\partial i}\right)^{-1}\left(v-Ri-\left(\frac{\partial\lambda(i,\theta)}{\partial\theta}\right)\frac{d\theta}{dt}\right)\right].dt \end{aligned} \tag{1}$$

$$T_m = J\frac{d^2\theta}{dt^2}+K_f\frac{d\theta}{dt}+T_s(\theta)$$

$$v-\left(\frac{\partial\lambda(i,\theta)}{\partial\theta}\right)\frac{d\theta}{dt}-\left(\frac{\partial\lambda(i,\theta)}{\partial i}\right)\frac{di}{dt}-Ri=0$$

$$\Rightarrow i(t)=\int\left[\left(\frac{\partial\lambda(i,\theta)}{\partial i}\right)^{-1}\left(v-Ri-\left(\frac{\partial\lambda(i,\theta)}{\partial\theta}\right)\frac{d\theta}{dt}\right)\right].dt$$

$$n(t)\triangleq\frac{d\theta}{dt}\Rightarrow n(t)=\int\left(J^{-1}(T_m-K_f n-T_s)\right).dt \tag{2}$$

Here, flux linkage, $\lambda(i,\theta)$, is a nonlinear function of current i and angular position θ . T_m , T_s and K_f denote the motor developed torque, the stiffness torque, and the frictional coefficient of air, respectively. $n(t)$ is the motor speed, and finally J is the moment of inertia of bundle of rotor and nozzle, [2].

Because of the small range of operation of θ (±3º), it can be assumed that T_m is directly proportional to current i, stiffness torque T_s is directly proportional to

position θ, and the differential term $\partial\lambda/\partial\theta$ is approximately constant. If the other differential term $\partial\lambda/\partial i$ is approximated to a constant value, then an acceptable linear model can be defined by the following equations:

$$v - K_b \frac{d\theta}{dt} - L\frac{di}{dt} - Ri = 0 \tag{3}$$

$$T_m = J\frac{d^2\theta}{dt^2} + K_f \frac{d\theta}{dt} + T_s \tag{4}$$

Where,

$$T_s = K_s\theta \tag{5}$$

$$T_m = K_t i \tag{6}$$

Substituting T_s and T_m from eqns. (5) and (6) into eqn. (4) gives

$$K_t i = J\frac{d^2\theta}{dt^2} + K_f \frac{d\theta}{dt} + K_s\theta \tag{7}$$

By substituting *i* from eqn. (7) into eqn. (3), the following equation is obtained:

$$\begin{aligned} &v - K_b\frac{d\theta}{dt} - L\frac{d}{dt}\left(\frac{J}{K_t}\frac{d^2\theta}{dt^2} + \frac{K_f}{K_t}\frac{d\theta}{dt} + \frac{K_s}{K_t}\theta\right) \\ &-R\left(\frac{J}{K_t}\frac{d^2\theta}{dt^2} + \frac{K_f}{K_t}\frac{d\theta}{dt} + \frac{K_s}{K_t}\theta\right) = 0 \end{aligned} \tag{8}$$

Consequently, the parametric transfer function of Laws' relay as a system input system output (SISO) can be derived in a third order form as in the following:

$$\begin{aligned} G(s) &= \frac{\theta(s)}{V(s)} \\ &= \frac{K_t/JL}{S^3 + \left(K_f/J + R/L\right)S^2 + \left((RK_f + K_bK_t + K_sL)/JL\right)S + RK_s/JL} \end{aligned} \tag{9}$$

4 Torque Motor Performance

Because of the low working frequency of 1 Hz for this servo-valve, the static characteristics have more important effect on dynamic performance compared to the typical ones used in aerospace equipment and optical scanning systems.

The measured magnitude of the magnetic stiffness torque for each position of shaft deflection in the range of ±3º is shown in Figure 2. It is obvious that this characteristic with a good approximation has a linear behavior, which confirms the linear coefficient of K_s. From the best linear curve fitting, the following value is obtained for this coefficient:

$$K_s = 1.1\,Nm/rad = 0.01921\,Nm/\deg \tag{10}$$

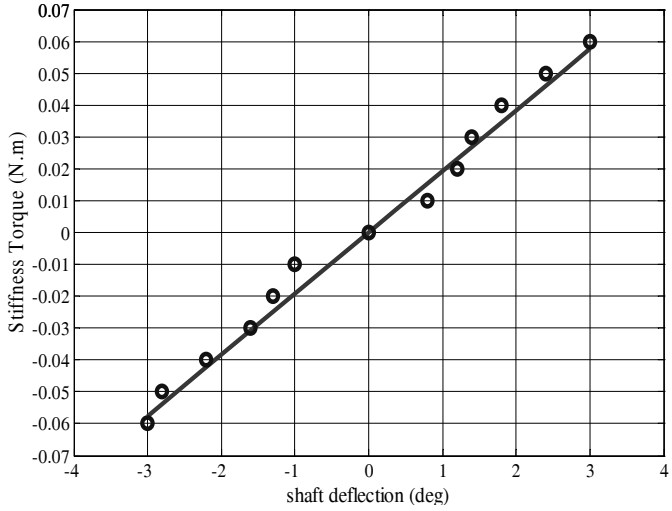

Figure 2
The measured stiffness torque characteristic and the best fit curve

The torque-current characteristic of the motor shown in Figure 3 has been obtained by exciting its coil with a variable DC source. The figure shows a good linear trend which again confirms the linear coefficient of K_t. From the best linear curve fitting, the following value is obtained for this coefficient:

$$K_t = 6.432\,Nm/A \tag{11}$$

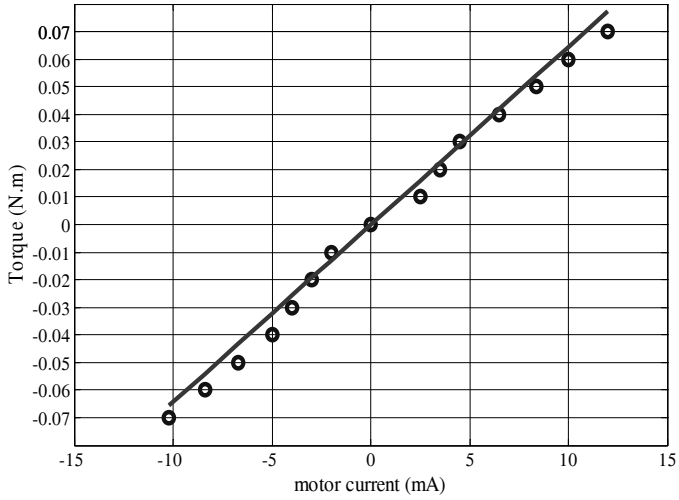

Figure 3

The measured torque-current characteristic and the best fit curve

Figure 4 presents the steady-state characteristic of the experimental LATM operating in the open loop conditions. The voltage-position characteristic demonstrates that with a desirable linear performance, the motor can be implemented in servo control systems.

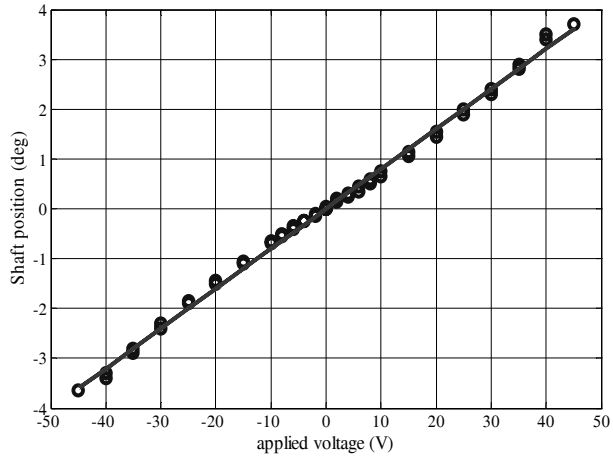

Figure 4

The measured voltage-position characteristic and the best fit curve

The approximately ideal characteristics of the designed parameters in Figures 3 and 4 present a good linear model for the controller design procedure. The measured parameters are summarized in Table 1.

Table 1
Measured parameters of available LATM

Torque constant $K_t\left(Nm/A\right)$	6.432
Back EMF constant $K_b\left(V.s/rad\right)$	0.08
Winding resistance $R(\Omega)$	3630
Winding inductance $L\left(H\right)$	34
Rotor inertia $J\left(kg.m^2\right)$	7.246×10^{-7}
Frictional coefficient $K_f\left(Nm.s/rad\right)$	2.7×10^{-4}
Magnetic stiffness $K_s\left(Nm/rad\right)$	1.1

A block diagram representation of the torque motor is shown in Figure 5 to illustrate the dynamic performance of its linear model. In this figure, the resistance R is measured directly from voltage and current measurements, the moment of inertia J is calculated accurately by SolidWorks software, and the winding inductance is approximately calculated based on analysis of the current flow of motor when excited with low frequency sinusoidal voltage. Figure 6 shows the sinusoidal input voltage and time-response waveforms of current and the position of motor at a frequency of 10 Hz.

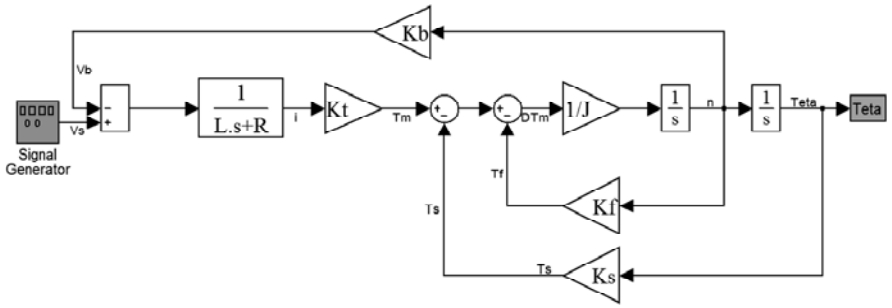

Figure 4
Block diagram of a LATM

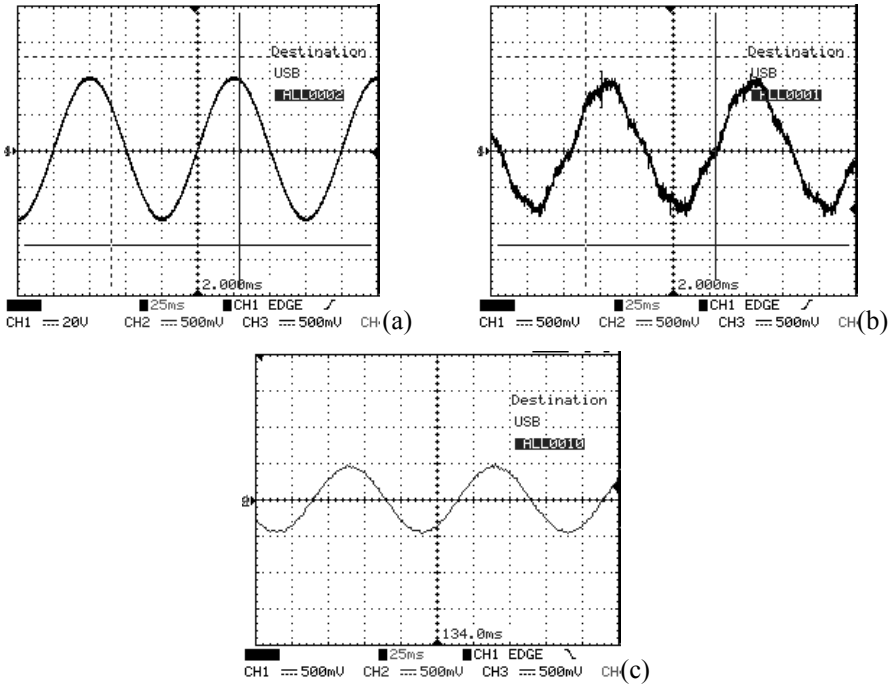

Figure 6

(a) 10Hz sinusoidal input, 40V peak (b) Time-response waveform of current (c) Time-response waveform of position

The frictional constant K_f, and back EMF coefficient K_b are difficult to measure directly. Hence, they are estimated from the predicted transfer function in the next section.

The experimental test system, consisting of the torque motor, a function generator with its output signal amplified by a voltage amplifier circuit, current sensor, and an arc type potentiometer fed by ±500 mV voltage with its wiper (contact arm) soldered to an arm linked to the motor shaft is shown in Figure 7.

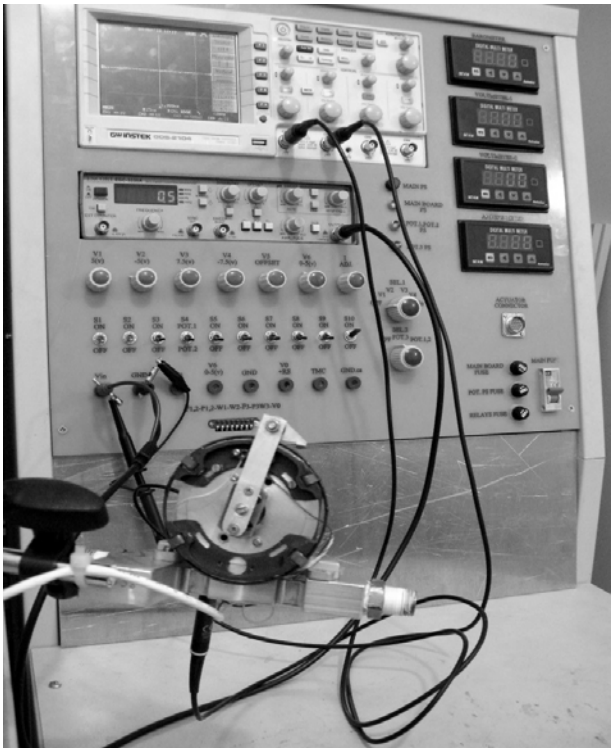

Figure 7
The experimental measurement system

5 Classical Identification

In linear time-invariant SISO dynamic systems, it is possible to derive the linear transfer function model by analyzing the response of the system to any forcing input. The step and frequency response tests are two common practical methods in classical identification [10]. The step response of a third-order system closely resembles to that of a first-order system with just tracking swings. According to the parsimony principle of model order determination [11], the simpler model can be chosen between two models with orders n_1 and n_2 ($n_1 > n_2$), if it adequately and accurately describes the system. However, in this case, because we consider the combined analytical and experimental models, it is necessary to choose the third-order model. Hence, by simultaneous analysis of step and frequency responses combined with trial and error procedure, the best third-order transfer function is obtained.

Figure 8 shows the variations of the rotor position in response to a step input voltage of 50 V in order to sweep the entire range of shaft deflection.

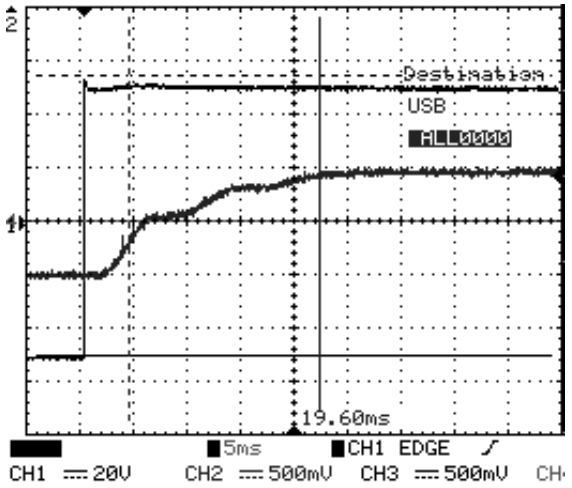

Figure 8
Variation of shaft deflection to a step input voltage of 50 V peak

Figures 9 and 10 show the measured characteristics of frequency and normalized step responses in comparison to the response of the estimated transfer function.

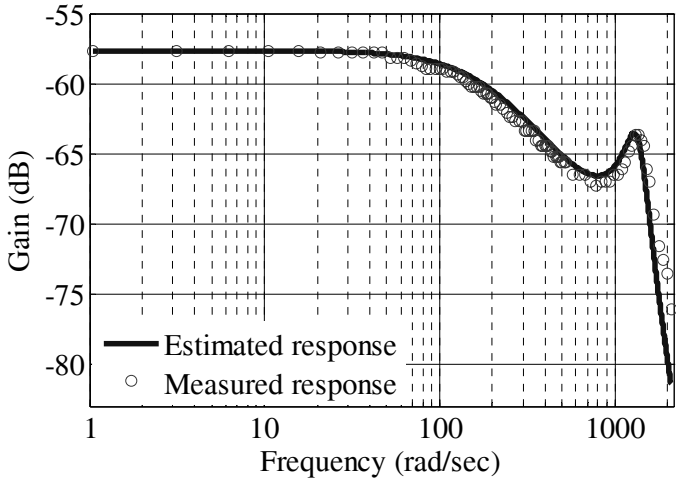

Figure 9
Measured and estimated frequency response chracteristics with input 40 V peak

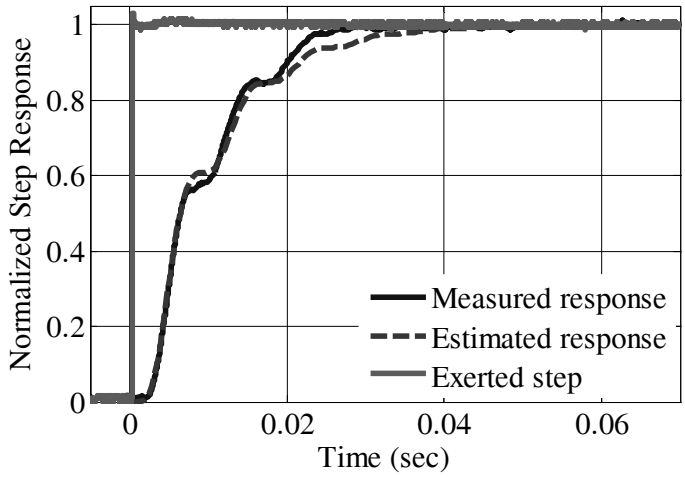

Figure 10
Normalized Measured and estimated step response chracteristics with input 40 V peak

Taking into account the response delay, the estimated transfer function is obtained as follows:

$$G(s)=\frac{\theta(s)}{V(s)}=\frac{241560.e^{-0.0011S}}{(S+120)\left(S^2+3356.5S+1537600\right)}$$

$$=\frac{241560.e^{-0.0011S}}{\left(S^3+492S^2+1582240S+184512000\right)} \qquad (12)$$

Assume that K_s, J and R are predetermined parameters. The remaining parameters, which are difficult to determine experimentally, are obtained by the comparison of the estimated transfer function of eqn. 12 with the parametric one from eqn. 9, and by solving the four linear equations. The estimated values of these parameters are shown in Table 2.

Table 2
Estimated values of the parameters by classical identification

$K_t\,(Nm/A)$	5.23
$K_b\,(V.s/rad)$	0.08
$L(H)$	29.9
$K_f\,(Nm.s/rad)$	2.7×10^{-4}

As is shown in Figure 11, the discrepancy between frequency responses of the system modeled by the estimated parameters and the measured parameters is adequately acceptable.

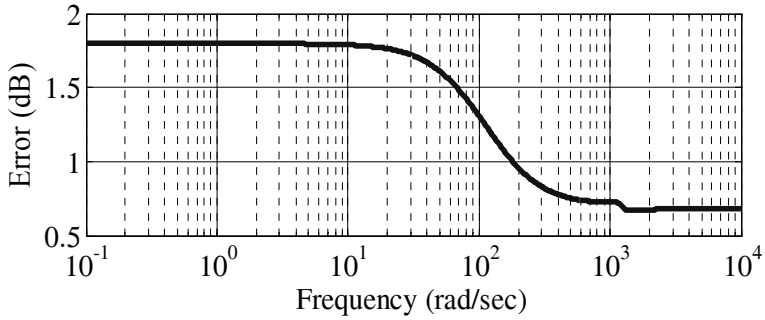

Figure 11

The error between the frequency responses of the system modeled by estimated and measured parameters

Conclusions

From a series of linear mathematical equations, a parametric third-order transfer function was achieved in order to model a pneumatic servo valve as a linear time-invariant SISO system. The static and dynamic performance characteristics of the torque motor were obtained by a test system. The results showed a remarkably good linear trend, which made it suitable for servo applications. Based on classical methods of identification, including frequency and step responses, an acceptable estimated model was fitted to the measured results. Finally, with the comparison of estimated and parametric third-order transfer functions, the design parameters of the servo-valve were obtained. The results were very close to the design specifications of the manufactured servo-valve, which validated the gray-box modeling.

References

[1] Igor L. Krivts, G. V. Krejnin: ’Pneumatic Actuating Systems for Automatic Equipment Structure and Design’ CRC Press, 2006

[2] S. Li, Y. Song: ’Dynamic Response of a Hydraulic Servo-Valve Torque Motor with Magnetic Fluids’, Mechatronics, Vol. 17, pp. 442-447, 2007

[3] Songjing Lia, W. Bao, "Influence of Magnetic Fluids on the Dynamic Characteristics of a Hydraulic Servo-Valve Torque Motor," Mechanical Systems and Signal Processing, Vol. 22, pp. 1008-1015, 2008

[4] I. R. Smith, J. G. Kettleborough, Y. Zhang: ’Simplified Modelling and Dynamic Analysis of a Laws' Relay Actuator’, Mechatronics, Vol. 9, pp. 463-475, 1999

[5] Y. Zhang, I. R. Smith, J. G. Kettleborough: 'Performance Evaluation for a Limited-Angle Torque Motor', IEEE/ASME Transactions on Mechatronics, Vol. 4, pp. 335-339, September 1999

[6] H. R. Bolton, Y. Shakweh: 'Performance Prediction of Laws' Relay Actuator', in IEE Conference on Electric Power Application, Vol. 137, Issue 1, 1990, pp. 1-13

[7] S. A. Evans, I. R. Smith, J. G. Kettleborough: 'Static and Dynamic Analysis of a Permanent Magnet Rectilinear Laws' Relay Actuator', in IEE Conference on Electric Power Application, Vol. 146, Issue 1, 1999, pp. 11-16

[8] S. A. Evans, I. R. Smith, J. G. Kettleborough: 'Permanent-Magnet Linear Actuator for Static and Reciprocating Short-Stroke Electromechanical Systems', IEEE/ASME Transactions on Mechatronics, Vol. 6, pp. 36-42, March 2001

[9] Ching Chih Tsai, Shui-Chun Lin, Hsu-Chih Huang, Yu-Ming Cheng: 'Design and Control of a Brushless DC Limited-Angle Torque Motor with its Application to Fuel Control of Small-Scale Gas Turbine Engines', Mechatronics, Vol. 19, Issue 1, 2009, pp. 29-41

[10] Ngoc Dung Vuong, Marcelo H. Ang Jr: 'Dynamic Model Identification for Industrial Robots', Acta Polytechnica Hungarica, Journal of Applied Sciences, Hungary, Vol. 6, Issue 5, pp. 51-68, 2009

[11] J. P. Norton: 'An Introduction to Identification' Academic Press Inc., 1986